Microwave Engineering
Ulm University

universität ulm

Ghost-Target Suppression in Coherent Radar Networks

David Werbunat, Benedikt Schweizer, Benedikt Meinecke, Rossen Michev, Jürgen Hasch, Christian Waldschmidt

DOI: 10.23919/EuRAD50154.2022.9784456

Ghost-Target Suppression in Coherent Radar Networks

David Werbunat#1, Benedikt Schweizer#, Benedikt Meinecke#,
Rossen Michev*, Jürgen Hasch*, Christian Waldschmidt#
#Institute of Microwave Engineering, Ulm University, 89081 Ulm, Germany
*Corporate Sector Research and Advance Engineering, Robert Bosch GmbH, 70465 Stuttgart, Germany.
1david.werbunat@uni-ulm.de

***Abstract*— Coherent radar-repeater networks offer great opportunities, e.g. in network-based direction of arrival (DoA) estimation. However, due to the special bistatic signal path with two reflections at the targets, the bistatic measurements are affected by additional ghost targets. The de-ghosting algorithm presented in this work not only allows for a mitigation of this additional ghost-targets but also the identification of unwanted clutter peaks. Thus, it enables the efficient exploitation of the network's possibilities, as verified by measurements.**

***Keywords*— Radar network, repeater, de-ghosting, clutter mitigation, bistatic radar, target identification.**

I. Introduction

From automotive to industrial applications, radar sensors are used to create a model of the sensor's surrounding. To improve the radar's resolution beyond the limits of classical multiple-input multiple-output (MIMO) radars, several radars can be combined to work cooperatively in a so-called radar network. This way measurements from different aspect angles may be combined. Furthermore, the evaluation of bistatic signals is possible, as one radar can evaluate the transmit signal from another radar after it was reflected at the targets.

A new kind of radar network exploiting the bistatic signals is the radar-repeater network [1], [2] exemplarily shown in Fig. 1. Instead of using multiple radars with their own signal evaluation, one MIMO radar sensor is combined with repeaters as additional network nodes. The repeater receive the signal from the radar after it was reflected at the targets, shift the signal by a low modulation frequency and retransmit it. After a second reflection at the target, the signal is received by the radar. Signal evaluation is performed exclusively at the radar, which results in simple hardware. Furthermore, phase coherency as well as cancellation of transmit (Tx) and receive (Rx) phase noise can be achieved without any hardware link between the network nodes, and even a phase based DoA estimation based on the large aperture of the network can be performed [1], [2], [3].

Precondition for the proper use of radar-repeater networks is the suppression of ghost-targets, which occur due to two paths from the radar to the repeater and back via the targets. Bistatic paths with the reflection at the same target on the way to the repeater and back result in the so-called single-target peaks, which are wanted for further evaluation. In contrast, the bistatic paths with reflections at different targets, as shown

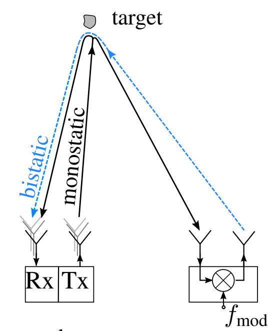

Fig. 1. Network concept of the radar repeater network. The monostatic path as well as the single-target path are exemplarily shown for one target. Figure based on [1].

in Fig. 2, are causing unwanted multi-target peaks in the range-velocity (Rv)-plot. Although there are known methods for the mitigation of multi-path peaks for single radars [4] and radar networks [5], [6], the issue of multi-target peaks in radar-repeater networks significantly differs from those.

Therefore, this work presents an algorithm capable of extracting the single-target peaks needed for further evaluation and separating them from the undesirable multi-target peaks. As clutter peaks do not correspond to the logic combination of single- and multi-target peaks, the algorithm furthermore allows to extract the clutter peaks from the true target peaks. As the whole algorithm works based on the target lists, it allows efficient de-ghosting and is applicable to orthogonal frequency-division multiplexing (OFDM) as well as frequency modulated continuous wave (FMCW) modulated radar-repeater networks [1], [2].

II. Rv-Evaluation in a Radar-Repeater Network

The processing of the monostatic and bistatic signals is performed at the radar. Using a FMCW radar, the monostatic Rv-evaluation does not differ from standard FMCW radar signal processing [7] with a direct evaluation of the intermediate frequency (IF)-signal by means of a 2D-fast Fourier transform (FFT). Only for the bistatic evaluation, the known frequency shift at the repeater has to be considered. This is done by a digital down-conversion of the Rx signal by the modulation frequency eliminating the Rv-shift caused by it. Then, the standard 2D-FFT-based evaluation is performed and—prior to the target extraction—the resulting radar image is cropped to the area where bistatic targets are expected. In the following, the bistatic ranges and relative velocities are based on the combination of the path between the radar and the target and the path between the target and the repeater and are referred to by R^{bi} and v^{bi}. In contrast, as for classical radar evaluation, the monostatic ranges R^{mono} and relative velocities v^{mono} are based on the path between radar and target only.

A. *Single-Target Peaks*

Due to the double path to and from the repeater via the same target, the bistatic single-target peaks are located approximately at twice the range and the velocity as the monostatic peak from the same target. Those single-target peaks contain the information about the path difference caused by the repeater position and the angle of the target, which may be exploited for a network based angle estimation [1], [2], [3], as well as the velocity difference due to the target's instantaneous velocity [8]. Therefore, these are the Rv-peaks wanted for further processing. In the following, the bistatic range and velocity of those peaks are notated as $R^{\mathrm{bi}}_{m,m} = 2R^{\mathrm{mono}}_{m} + 2\Delta R_m$ and $v^{\mathrm{bi}}_{m,m} = 2v^{\mathrm{mono}}_{m} + 2\Delta v_m$, respectively, where $m \in \{1, \ldots, N_{\mathrm{target}}\}$ is the index of the dedicated target. The offsets ΔR_m and Δv_m stem from the different aspect angles of the radar and the repeater.

B. *Multi-Target Peaks*

The multi-target peaks are caused by the signal paths with reflections at different targets on the way to the repeater and back, as exemplary shown in Fig. 2. Although those peaks may be useful in order to extract even further target information in future, it is crucial not to mistake them as single-target peaks.

In the following, the range and velocity of the multi-target peaks are notated as $R^{\mathrm{bi}}_{m,n}$ and $v^{\mathrm{bi}}_{m,n}$ with $m, n \in \{1, \ldots, N_{\mathrm{target}}\}$, $n \neq m$. Their relation to the single-target peaks is given by

$$\begin{aligned} R^{\mathrm{bi}}_{m,n} &= R^{\mathrm{bi}}_{n,m} = 0.5R^{\mathrm{bi}}_{m,m} + 0.5R^{\mathrm{bi}}_{n,n} \\ v^{\mathrm{bi}}_{m,n} &= v^{\mathrm{bi}}_{n,m} = 0.5v^{\mathrm{bi}}_{m,m} + 0.5v^{\mathrm{bi}}_{n,n}. \end{aligned} \tag{1}$$

Thus, they are based on a linear combination of the single-target peaks, leading to one multi-target peak in between every two single-target peaks. In total, this results in an amount of

$$N_{\text{multi-target}} = \sum_{k=0}^{N_{\text{target}}-1} k \tag{2}$$

multi-target peaks in every bistatic Rv-plot. Additionally, there may occur multi-target peaks based on the combination of one weak and one strong target, where the single-target peak of the weak target is not detectable.

III. Peak Identification

Prior to the identification of the Rv-peaks, their detection is mandatory. This is done by an ordered-statistic constant false-alarm rate (OS-CFAR) [9] and an algorithm extracting

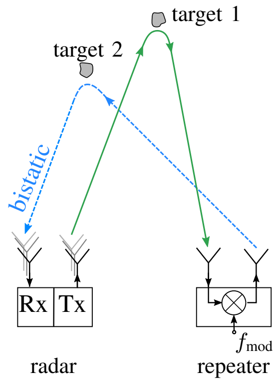

Fig. 2. Multi-target path in a radar-repeater network.

the local maxima, each performed separately for the monostatic and every bistatic evaluation. Then, the further identification is based on the resulting mono- and bistatic target lists. For the peak identification, the relation between single-target peaks and multi-target peaks from (1) is exploited. However, to do so, at least one bistatic peak has to be identified as single-target peak. This peak in the following is called reference peak.

A. *Reference Peak*

The reference peak is the starting point for the further target identification. Thus, its proper selection is crucial, which is done based on a comparison of the mono- and the bistatic target list by Algorithm 1.

Algorithm 1 Reference Peak

Input: Mono- and bistatic Rv-peaks, sorted by their power
Output: Reference peak pair p_{ref}, s_{ref}

$p_{\mathrm{ref}} = 0$
$s_{\mathrm{ref}} = 0$
$p = 1$
while $p \leq N^{\mathrm{mono}}_{\mathrm{peak}}$ & $p_{\mathrm{ref}} = 0$ **do**
  if p fulfills (3) **then**
    $s = 1$
    while $s \leq N^{\mathrm{bi}}_{\mathrm{peak}}$ & $s_{\mathrm{ref}} = 0$ **do**
      if s, p fulfill (4) **then**
        if s fulfills (5) **then**
          $p_{\mathrm{ref}} = p$
          $s_{\mathrm{ref}} = s$
        end if
      end if
      $s = s + 1$
    end while
  end if
  $p = p + 1$
end while

To start with, the target lists are sorted by decreasing peak power, as peaks with more signal power are expected to be more reliable. If necessary, the monostatic peak from the radar overcoupling can be excluded by applying a range threshold. Then, the algorithm iteratively searches for a monostatic peak that has a distance of $\Delta R_{\min}$ and $\Delta v_{\min}$, respectively, to any other of the $N_{\text{peak}}^{\text{mono}}$ monostatic peaks and thus satisfies

$$\begin{aligned} &\left|R_q^{\text{mono}} - R_p^{\text{mono}}\right| > \Delta R_{\min} \\ &\left|v_q^{\text{mono}} - v_p^{\text{mono}}\right| > \Delta v_{\min}\ \forall q \in \{1, \dots, N_{\text{peak}}^{\text{mono}}\},\ q \neq p. \end{aligned} \tag{3}$$

After finding a proper monostatic peak, the matching bistatic peak has to be found. As the bistatic path has approximately twice the length and twice the Doppler frequency than the monostatic one, a bistatic peak $s \in \{1, \dots, N_{\text{peak}}^{\text{bi}}\}$ fulfilling

$$\begin{aligned} &\left|R_s^{\text{bi}} - 2R_p^{\text{mono}}\right| < \epsilon_R \\ &\left|v_s^{\text{bi}} - 2v_p^{\text{mono}}\right| < \epsilon_v \end{aligned} \tag{4}$$

has to be found. $N_{\text{peak}}^{\text{bi}}$ is the total number of bistatic peaks. The maximal deviations ϵ_R and ϵ_v have to be selected properly—when chosen too high, a wrong peak may be picked as match, when chosen too small, the correct peak may not be found, as deviations due to the different aspect angles of the radar and the repeater are expected. After finding a bistatic match, the distance to any other bistatic peak is checked. If there are other peaks close by, they might get mistaken. Thus, peak s must fulfill

$$\begin{aligned} &\left|R_s^{\text{bi}} - R_u^{\text{bi}}\right| > \Delta R_{\min} \\ &\left|v_s^{\text{bi}} - v_u^{\text{bi}}\right| > \Delta v_{\min}\ \forall u \in \{1, \dots, N_{\text{peak}}^{\text{bi}}\},\ u \neq s. \end{aligned} \tag{5}$$

If all conditions are satisfied, a reference pair of a monostatic and a bistatic peak is found.

B. Bistatic Target Peak Identification

With the reference target, one single-target peak is already known. Starting from this, Algorithm 2 tests for every other bistatic Rv-peak x, whether multi-target peaks occur between this peak and the reference peak s_{ref}.

Algorithm 2 Bistatic Target Peak Identification

Input: Mono- and bistatic Rv-peaks sorted by their power, reference peak pair
Output: Peak information

```
x = 1
while x ≤ N_peak^bi do
    u = 1
    while u ≤ N_peak^bi do
        if x, u fulfill (7) then
            peak x is single-target peak
            peak u is multi-target peak based on s_ref and x
        end if
        u = u + 1
    end while
    x = x + 1
end while
```

At first, based on the the range and velocity of the reference peak s_{ref} and the peak u, a test range $R_{s_{\text{ref}},u}^{\text{bi}}$ and test velocity $v_{s_{\text{ref}},u}^{\text{bi}}$ are analogously to (1) calculated as

$$\begin{aligned} R_{s_{\text{ref}},u}^{\text{bi}} &= 0.5R_{s_{\text{ref}}}^{\text{bi}} + 0.5R_u^{\text{bi}} \\ v_{s_{\text{ref}},u}^{\text{bi}} &= 0.5v_{s_{\text{ref}}}^{\text{bi}} + 0.5v_u^{\text{bi}}. \end{aligned} \tag{6}$$

Then, every bistatic peak $x \in \{1, \dots, N_{\text{peak}}^{\text{bi}}\}$, $x \neq u$ is tested to see if it is the multi-target peak of the reference s_{ref} and the peak u, i.e. if it fulfills

$$\begin{aligned} &\left|R_x^{\text{bi}} - R_{s_{\text{ref}},u}^{\text{bi}}\right| < \epsilon_R \\ &\left|v_x^{\text{bi}} - v_{s_{\text{ref}},u}^{\text{bi}}\right| < \epsilon_v. \end{aligned} \tag{7}$$

If a peak x can be found, peak u is a single-target peak and thus relevant for further evaluation. In the next step, the corresponding monostatic target can be searched. This way, all peaks can be tested and the single-target peaks can be extracted.

Even though theoretically one single reference target is sufficient to identify all single-target peaks, there may be false positives when another target peak or a clutter peak occurs where the multi-target peak is expected. The results can be further improved by iteratively repeating Algorithm 2, each iteration with a new reference target. The first iteration is performed with the reference target found by Algorithm 1. Then, for the bistatic peaks being identified as a single-target peak, a corresponding monostatic peak is searched for which satisfies (4). These two peaks can be used as a new reference peak pair. This is repeated, until all proper single-target peaks have been used as reference peaks.

In the next step, the results from the different iterations are combined. The simplest way is to check if the peak was identified as a single-target peak more often than it was not. For further improvements, it is also possible to weight the iterations. Thus, the single target peaks are identified and can be separated from the unwanted multi-target and clutter peaks.

IV. Measurements

For measurements, a 77 GHz FMCW radar using a bandwidth of 2 GHz and 512 ramps with a repetition time of 0.22 ms is combined with a repeater similar to the one described in [10]. The time delay due to the repeater hardware is corrected based on a calibration. The repeater is placed laterally to the radar at a distance of 24 cm. The measurements are set up in an anechoic chamber, which leads to a controlled target scenario. The scenario shown in Fig. 3 contains a metal rod at 1.17 m, a corner reflector at 3.89 m, and, as moving targets, four metallic cylinders placed on a rotating platform centered at 2 m.

Fig. 4 shows the monostatic measurement result. In addition to the targets, various clutter occurs, which very likely is caused by multi-reflections between the targets.

The bistatic Rv-plot is shown in Fig. 5. It has to be considered that the range and velocity is referring to R^{bi} and v^{bi}, thus including the path between the radar and the target as well as the path between the repeater and the target. All peaks extracted by the OS-CFAR algorithm [9] are marked in the bistatic Rv-evaluation, which does not only include the single-target peaks and the multi-target peaks but also unwanted clutter peaks.

In Fig. 5a, the result of the peak identification after the first iteration is shown. As reference peak, by Algorithm 1 the corner reflector has been chosen, as this targets provides a

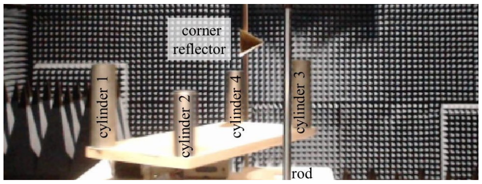

Fig. 3. Measurement scenario.

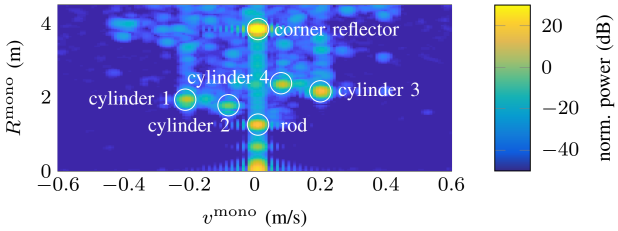

Fig. 4. Monostatic Rv-evaluation.

high signal power. Already in this first iteration all single-target peaks are identified. However, two of the clutter peaks, which are marked as false positives in Fig. 5a, where also identified as single-target peaks.

After six iterations, all targets from the scenario have been used as reference peaks, the false positives are corrected, and only some wrongly identified multi-target peaks remain. The result is shown in Fig. 5b. Thus, all relevant peaks are successfully extracted and separated from clutter and multi-target peaks, showing the good performance of the algorithm even in a scenario with multiple targets close to each other.

V. Conclusion

In radar-repeater networks, multi-target peaks are an unavoidable issue caused by additional signal paths with reflections at different targets on the way to the repeater and back. However, with the algorithm presented in this paper, it is possible to extract the relevant single-target peaks from the unwanted peaks. This way, not only this limitation of such networks can be overcome but also the identification of clutter peaks is feasible. Thus, as verified by measurements, the algorithm offers an efficient single-snapshot based method for de-ghosting of the bistatic target list.

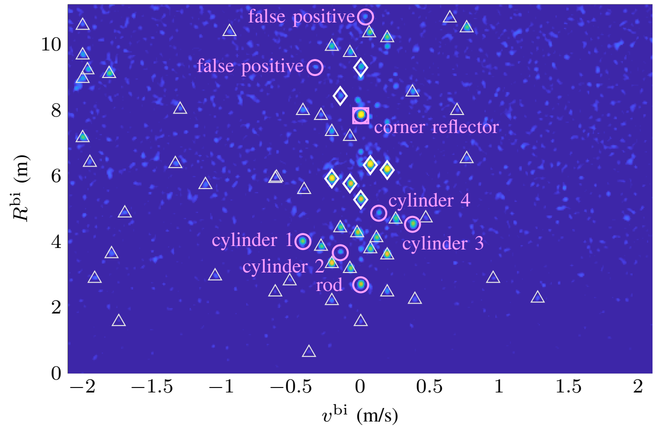

(a) Peak identification after one iteration of Algorithm 2.

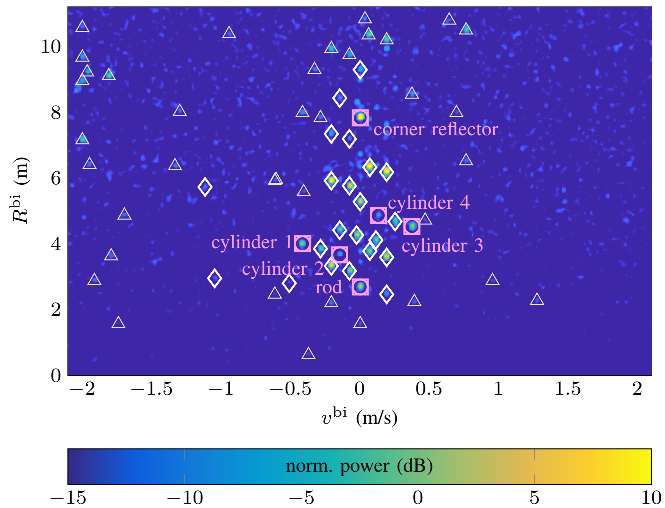

(b) Peak identification after six iterations of Algorithm 2.

Fig. 5. Bistatic Rv-evaluation. All peaks extracted by the OS-CFAR are marked based on their identification from Algorithm 2 (□: Peak used as reference peak; ○ :Single-target peak; ◇: Multi-target peak; △: Unknown peak). Parameters: $\epsilon_R = \Delta R_{\text{min}}/2 = 0.15\,\text{m}$; $\epsilon_v = \Delta v_{\text{min}}/2 = 0.035\,\frac{\text{m}}{\text{s}}$.

References

[1] D. Werbunat, B. Meinecke, B. Schweizer, J. Hasch, and C. Waldschmidt, "OFDM-based radar network providing phase coherent DOA estimation," *IEEE Trans. Microw. Theory Techn.*, vol. 69, no. 1, pp. 325–336, 2021.

[2] B. Meinecke, M. Steiner, J. Schlichenmaier, J. Hasch, and C. Waldschmidt, "Coherent multistatic MIMO radar networks based on repeater tags," *IEEE Trans. Microw. Theory Techn.*, vol. 67, no. 9, pp. 3908–3916, 2019.

[3] D. Werbunat, B. Meinecke, M. Steiner, and C. Waldschmidt, "Phase recovery in sensor networks based on incoherent repeater elements," in *Proc. IEEE MTT-S Int. Microwave Symp.*, 2020, pp. 1149–1152.

[4] G. Gennarelli and F. Soldovieri, "Multipath ghosts in radar imaging: Physical insight and mitigation strategies," *IEEE J. Sel. Topics Appl. Earth Observ. Remote Sens.*, vol. 8, no. 3, pp. 1078–1086, 2015.

[5] A. Samokhin, I. Ivashko, and A. Yarovoy, "Algorithm for multiple targets localization and data association in distributed radar networks," in *15th Int. Radar Symp. (IRS)*, 2014, pp. 1–6.

[6] H. Li, G. Cui, S. Guo, L. Kong, and X. Yang, "Target tracking and ghost mitigation based on multi-view through-the-wall radar imaging," in *IEEE Radar Conf.*, 2020, pp. 1–5.

[7] V. Winkler, "Range Doppler detection for automotive FMCW radars," in *Eur. Radar Conf.*, 2007, pp. 166–169.

[8] B. Meinecke, M. Steiner, J. Schlichenmaier, and C. Waldschmidt, "Instantaneous target velocity estimation using a network of a radar and repeater elements," in *16th Eur. Radar Conf. (EuRAD)*, 2019, pp. 241–244.

[9] S. Blake, "OS-CFAR theory for multiple targets and nonuniform clutter," *IEEE Trans. Aerosp. Electron. Syst.*, vol. 24, no. 6, pp. 785–790, 1988.

[10] M. S. Dadash, J. Hasch, P. Chevalier, A. Cathelin, N. Cahoon, and S. P. Voinigescu, "Design of low-power active tags for operation with 77-81-GHz FMCW radar," *IEEE Trans. Microw. Theory Techn.*, vol. 65, no. 12, pp. 5377–5388, 2017.